ARCHIVES OF ELECTRICAL ENGINEERING VOL. 68(4), pp. 771–786 (2019)

DOI 10.24425/aee.2019.130682

Investigation on ferroresonance due to power transformer energization in high voltage 400 kV transmission grid

MATEUSZ POLEWACZYK, SYLWESTER ROBAK, MARCIN SZEWCZYK

Institute of Electrical Power Engineering, Warsaw University of Technology
Koszykowa 75 Str, 00-662 Warsaw, Poland
e-mail: mateusz.polewaczyk@ien.pw.edu.pl

(Received: 11.02.2019, revised: 27.05.2019)

Abstract: This paper presents a study on ferroresonance occurring in a high voltage 400 kV transmission grid due to energization of power transformer under no-load conditions. The system scenarios analyzed in the present paper are considered as critical for development and modernization plans as currently announced by the national grid operator in Poland. The PSCAD simulation model was developed and applied for several study cases of a system with double-circuit arrangement of a transmission line. It is shown that the ferroresonant oscillations can be initiated by two-phase switching operation of a line circuit breaker. The impact of the double-circuit length on the ferroresonance mode and severity is demonstrated with the use of the Poincaré map analysis and Short Time Fourier Transform. It is demonstrated that the length of the transmission line that is mutually coupled in the double-circuit arrangement has a significant impact on the ferroresonance occurrence and on its mode. As the ferroresonance can pose severe threat to the power system components due to the severe overvoltage and overcurrent oscillations, the analysis presented in this paper demonstrates the necessity of the ferroresonance analyses for any re-designed transmission system.

Key words: ferroresonance, high voltage, Poincaré map, power system transients, PSCAD

1. Introduction

Ferroresonance is a transient or continuous phenomenon that can occur in power grids in which interaction between nonlinear inductive components and capacitive elements is involved [1]. When these elements are connected in series, the unusual oscillations of voltages, and when connected in parallel – the unusual oscillations of currents, can occur [2]. The oscillations exceeding ratings

of components pose a severe threat to power system components due to the generated overvoltages and overcurrents. Although well understood in nature, the ferroresonance phenomenon attains a constant interest among researchers due to the ongoing development of power grid structure and components [3]. In the changing system conditions, ferroresonance can be a major cause of system maloperation and even severe faults of power system components, such as voltage dividers or even power transformers and reactors, as reported in [4] for distribution grids and in [5] for transmission grids.

Investigating ferroresonance is a challenging task primarily due to the high number of factors that can have an impact on the ferroresonance occurrence, and due to high sensitivity of the phenomenon on relatively small changes of the power grid parameters [6]. Variety of research papers have been published on the topic, presenting analyzes on: transformer/grading-capacitor circuit operation and its impact on the ferroresonance phenomenon [7], investigation of different system conditions for ferroresonance occurrence [8], impact of the ferroresonance phenomenon on operating performance of power transformers [9], double-circuit transmission line arrangement and its impact on the ferroresonance occurrence in de-energized transformer through capacitive coupling of power lines [10]. These aspects, although extensively addressed in the literature, remain vital due to the presently widely expressed needs for development and modernization of existing power system infrastructure. As the changing power system infrastructure influences ferroresonance conditions, the study cases of new system topologies, as well as the methods on the ferroresonance analyses are being investigated [11–14]. The analyzes are being conducted via numerical simulations with the use of dedicated simulation models of the power grid components.

The present paper contributes to the research on ferroresonance phenomenon by (a) performing ferroresonance study on transmission circuit characterized by typical parameters of a modern 400 kV power grid, (b) testing of the impact of double-circuit transmission line tower construction on ferroresonance (which currently is one of the major development schemas to increase transmission capability of power corridors), (c) proposing a model for testing of various ferroresonance systems allowing determination of parameters of a critical impact on the ferroresonance in different system variants.

In this paper, the ferroresonance phenomenon is investigated with respect to high voltage 400 kV power grid in Poland. The methods of ferroresonance analysis are characterized as applied to a typical example of a 400 kV power grid, for which simulation results are reported. The study was performed for two constructions of HV transmission line towers with the use of the commercial PSCAD simulation software.

2. Principle characterization of ferroresonance

Ferroresonance is defined as a phenomenon initiated by the interaction of power system capacitive and nonlinear inductive components. The nonlinear inductance is typically assigned to magnetic cores of conventional voltage transformers however it can also be related to the magnetic cores of a power transformer or reactors. The phenomenon typically results in very high overvoltages or overcurrents that can pose a severe threat to power system operation or can be a root cause of power components faults. An example of a principal ferroresonance circuit is shown in Fig. 1. In the diagram, the capacitances C_{se} and C_{sh} represent equivalent series and shunt

capacitances of the power system, e_{PS} is the power system supply voltage, R_m is the equivalent resistance corresponding to magnetic circuit losses, $L(\phi)$ is the magnetizing inductance. The magnetization curve of the inductance for the ferroresonance analysis can be modeled by two linear characteristics or with a polynomial representation as follows:

$$i_L(\phi) = a\phi + b\phi^q, \tag{1}$$

where term $a\phi$ represents the linear part of the curve and $b\phi^q$ represents the saturation effect of the core.

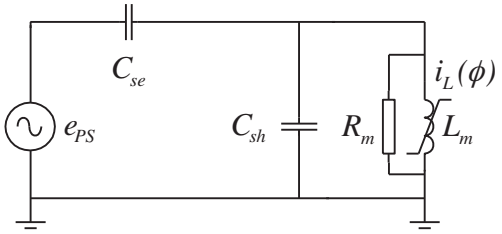

Fig. 1. Ferroresonance circuit

The dynamics of the circuit shown in Fig. 1 is described by the following nonlinear differential equation:

$$\frac{\mathrm{d}^2\phi}{\mathrm{d}t^2} + \frac{1}{R_m(C_{se+}C_{sh})}\frac{\mathrm{d}\phi}{\mathrm{d}t} + \frac{1}{(C_{se+}C_{sh})}i_L(\phi) = \frac{C_{se}}{(C_{se}+C_{sh})}\frac{\mathrm{d}e_{PS}}{\mathrm{d}t}. \tag{2}$$

The major difference between ferro- and linear-resonance is that the latter one may occur only when excited with a specific frequency, while the ferroresonance can occur for many frequencies depending on the operating point on the magnetization curve of the inductive element. For the initiation of the linear resonance it is thus required to adjust the frequency of the driving source to the resonance frequency of the system. For the ferroresonance, the oscillations can be also initiated throughout the voltage change, with the frequency of the driving source remained unchanged. The ferroresonance is thus a complex non-linear phenomenon, which occurrence and severity depends on several factors [15]:

a) circuit parameters (resistance and capacitance),
b) supply conditions (variation of the voltage magnitude and supply frequency),
c) magnetic material characteristics.

The conditions that can lead to the occurrence of the ferroresonance in a power system include [16]: significant rated voltages in the system, energizing of transformers under no-load conditions or during small-load operation, energizing of transformers with un-earthed neutral, connecting systems to cable lines, connecting systems with a small short-circuit impedance, connecting transformers with small losses in the core, connecting a single phase or two phases of three-phase circuits. All of these system conditions introduce significant change in either supply voltage or inductive/capacitive system parameters.

2.1. Classification of ferroresonance systems

For HV transmission grids the ferroresonance phenomenon is assigned to two main system configurations: 1) with voltage transformers and 2) with power transformers (or inductive shunt reactors).

The ferroresonant circuits with the voltage transformers pertain only to inductive voltage transformers (as the capacitive voltage transformers are equipped with ferroresonance suppression circuits). For HV transmission grids the ferroresonant circuit refers to the inductive voltage transformer energized through the voltage grading capacitance of open circuit breakers.

The ferroresonance in systems with the power transformers may occur in the situations where the power transformer is [17, 18]:

– supplied accidentally on one or two phases,
– supplied through a long transmission line with low short-circuit power,
– connected to a series compensated transmission line,
– connected to a deenergized transmission line running in parallel to the energized line(s).

The ferroresonance phenomenon in a system with an asymmetrical connection of the power transformer may occur when two parts of the system are being connected to or disconnected from one or two phases only. In such a situation the ferroresonance can occur when the load of the transformer is very low (or for no-load condition) and when the capacitance between the transformer and the feeding node is sufficiently high.

Ferroresonance in systems with transformers operating in no-load condition can occur when the supply voltage is fed from the source with a low short-circuit capacity and when the transformer is connected to the grid through a long transmission line. Such conditions can occur in post-blackout system restitution during sending of low energy to distant customers.

For systems of multi-circuit configuration, involving also power transformers, the ferroresonance can occur when one circuit is being energized while the second one is deenergized. For such systems the connection between circuits is constituted by the mutual capacitance between the circuits involved. In such system configuration the following factors may lead to the ferroresonance occurrence: absence or failure of a circuit breaker and presence of a certain section of a multi-circuit transmission line with mutual capacitance between circuits. An example of the ferroresonance system with mutual capacitance and a power transformer is presented in the Fig. 2.

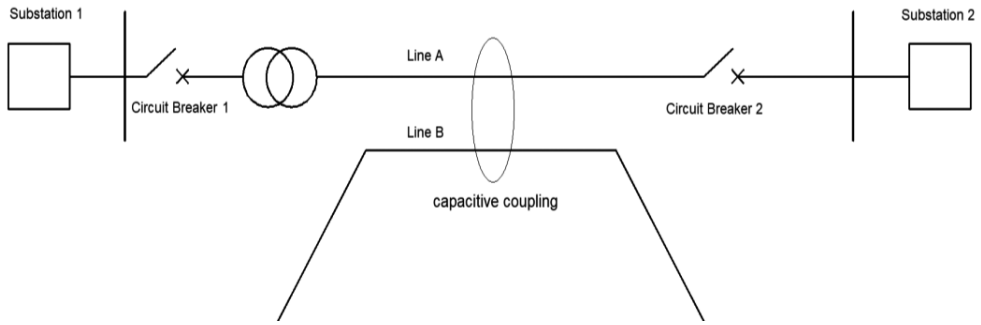

Fig. 2. Example of ferroresonance system with transformer and mutual coupling of circuits in multi-circuit transmission lines

3. Ferroresonance in power grids

Research on a ferroresonance phenomenon in power grids can be grouped into the following areas depending on the type of analysis:

- detection of the ferroresonance based on the chaos theory and then analysis of nonlinear dynamic system behavior with the use of bifurcation diagrams, Poincaré maps, or phase planes – this approach allows one to identify the ferroresonance stability area with respect to dynamics variation of the system parameters and its initial conditions [19],
- modeling of ferroresonant systems focusing on nonlinear inductive components – this involves modeling of magnetic cores of power transformers and reactors, including hysteresis effects [20],
- investigations on ferroresonance occurrence in power grids [21]:
  a) experimental research on scaled down physical models of the system and components,
  b) research on ferroresonant waveforms obtained from full scale measurements in power grids,
- investigation on system configurations that should be used to avoid ferroresonance occurrence as well as development of new mitigation methods on ferroresonance effects [22],
- signal processing methods for analyzing ferroresonance voltage or current waveforms [23–25]:
  a) Short Time Fourier Transform (STFT),
  b) wavelet transform,
- parametric and statistical analyses of ferroresonance parameters jointly with the analysis of investigated system parameters [23].

4. Methods of identification and classification of ferroresonance

The following methods are in use for analyzing the ferroresonance phenomenon in order to identify and classify the phenomenon type and severity:

- Short Time Fourier Transform (STFT) – this method is being used for analyzing the frequency spectrum of the ferroresonant voltage and current waveforms,
- Poincaré maps are being used to analyze the stroboscopic images calculated for the measured or simulated ferroresonant voltage and current waveforms in voltage-current (v–i) or voltage-flux (v–ϕ) domains,
- wavelet transform,
- analysis of power energy quality factors.

In this paper the ferroresonance phenomenon in a typical modern 400 kV high voltage electrical grid is presented. For the analysis the STFT and the Poincaré maps have been used. Identification of the ferroresonance by means of the power energy quality factors is reported in [26, 27], whereas the application of the wavelet transform is reported in [25].

4.1. Ferroresonance analysis with Short Time Fourier Transform (STFT)

Short Time Fourier Transform (STFT) allows one to analyze frequency components of a given time-domain waveform together with the frequency component evolution over the time of the analyzed process. The voltage and the current waveforms occurring in the power system due to the ferroresonance are of transient nature (i.e. with time-varying waveforms' shapes). The time-domain analysis of long records of such waveforms can lead to significant loss of information on the time variation of the waveforms parameters. Frequency domain analysis of consecutive parts of the analyzed waveforms according to the STFT procedure, allows for the preservation of all information on frequency components and their evolution over the time. Segments of the time domain waveforms are being extracted with the use of the so-called window function, denoted below as $g(t)$. Each segment, as extracted with the window function $g(t)$, is then integrated to provide the Fourier transform over the time. The time length of the segment allows selection of proper resolution in both time and frequency domains.

The STFT is defined with the following formula [23]:

$$X(\tau, f) = \int_{-\infty}^{+\infty} x(t) g(t-\tau) \exp(-j2\pi f t)\, \mathrm{d}t, \tag{3}$$

where: $x(t)$ is the investigated time domain waveform, $g(t)$ is the window function (time-domain segment of the analyzed signal), τ is the midpoint of the given time window (position of the window function $g(t)$ over the time axis).

In the case of the Discrete Fourier Transform (DFT), the STFT is given by the following formula [23]:

$$X(m, f) = \sum_{n=-\infty}^{+\infty} x(n) g(n-m) e^{j\omega n}, \tag{4}$$

where: $x(n)$ is the analyzed signal, $g(n)$ is the window function (time-domain segment of the analyzed signal).

4.2. Ferroresonance analysis with Poincaré maps

Poincaré maps serve as a convenient method to describe the time domain waveforms of highly dynamic processes, of the type such as power system transients.

The nonlinear systems can be described by means of the matrix of differential equations [28]:

$$\frac{\mathrm{d}x}{\mathrm{d}t} = f(t, x), \tag{5}$$

where: x is the state space variable vector, t is the time of the analyzed process.

The vector x_T as calculated for the time instance $t = T$ is given by the integral for the time range of T from the initial value given by x_0 [28]:

$$x_T = \int_0^T f(\tau, x(\tau))\, \mathrm{d}\tau + x_0\,. \tag{6}$$

Graphical representation of the Poincaré map is shown in Fig. 3. In the case of the waveforms with no transient components, the state space variables for two boundary conditions (at $t = 0$ and at $t = T$) are equal, which can be presented as:

$$x_T = P(x_0) = x_0, \tag{7}$$

where: $P(\ )$ is a function representing the relation between x_T and x_0. The $P(x_0)$ is typically a nonlinear function of x_0.

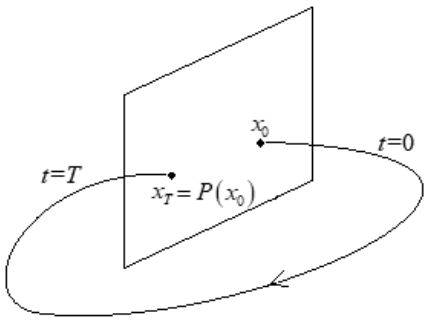

Fig. 3. Graphical representation of Poincaré map, based on [28]

For application in ferroresonance studies, Poincaré maps are created in a way to depict in each frequency period of the analyzed waveform the highest instantaneous values of the analyzed voltage waveforms jointly with the respected values of the current waveforms.

Fig. 4 shows examples of waveforms that are typically observed for ferroresonance in power grids. The waveforms are presented jointly with respective Poincaré maps that allow for classification of the ferroresonance type (as given in the figure).

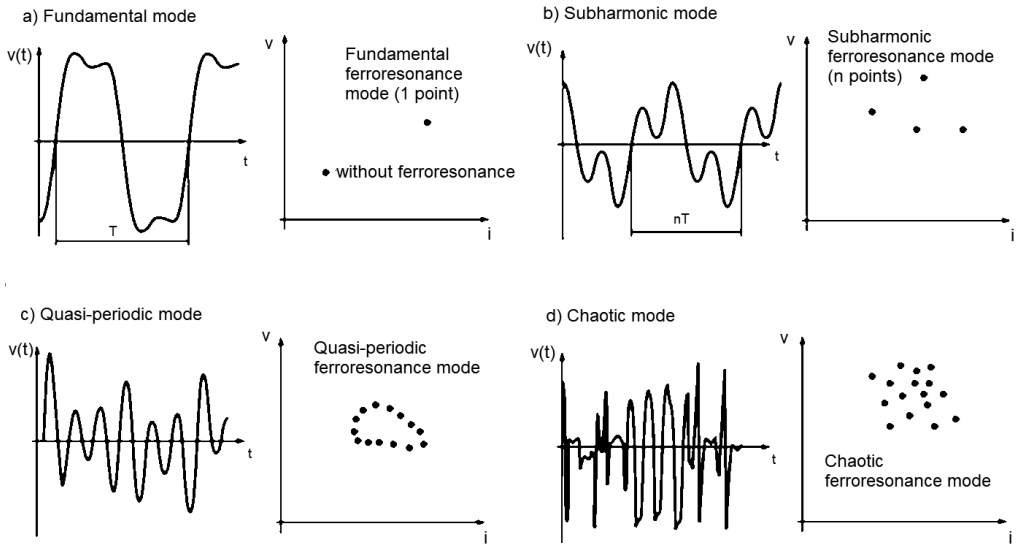

Fig. 4. Examples of voltage waveforms during ferroresonance with relevant Poincaré maps with the ferroresonance modes indicated, based on [29]

5. Simulation model used for ferroresonance study of 400 kV high voltage transmission grid

The simulation model presented in this paper was developed for the purpose to investigate the ferroresonance phenomenon in power grid configurations that are typical for the ferroresonance occurrence. For the model development a test system configuration was assumed as outlined below.

The following ferroresonant configurations in the test system were investigated:

– a power transformer is supplied with one or two phases only,
– a power transformer is supplied through a long overhead transmission line with low short-circuit power,
– a power transformer is connected to a de-energized transmission line running in parallel with an energized line.

The simulations presented in this paper were conducted with the use of the PSCAD simulation software [30].

5.1. Test system

Fig. 5 shows a simplified diagram of a typical high voltage 400 kV test system as assumed in this paper for the ferroresonance study. The system consists of two 400 kV transmission lines (A and B, see Fig. 5). The lines are mutually coupled in the double-circuit system at the distance between points B2 and B3. The two transmission lines, Line A and Line B, are operated in unloaded condition. Line B is terminated with an autotransformer of 330 MVA that is operated in no-load condition. Table 1 summarizes parameters of the assumed test system. Each of the line is supplied with a separate system node (node B1 at short-circuit power of S''_K = 3 GVA, and node B5 at short-circuit power of S''_K = 1 GVA.

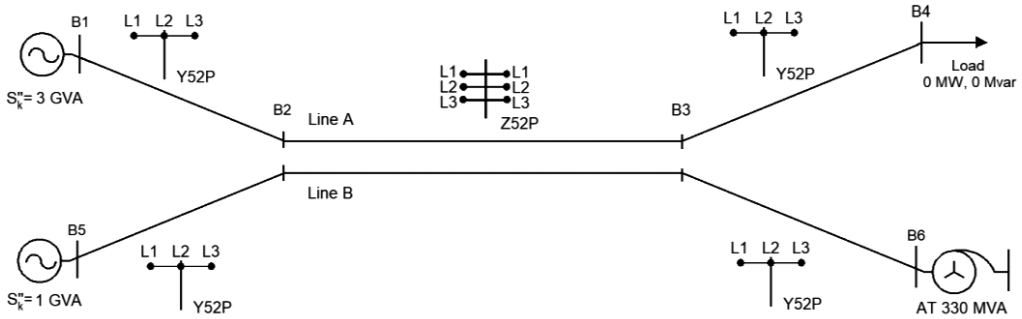

Fig. 5. Simplified diagram of investigated test system for analysis of ferroresonance phenomenon

For modeling of the transmission lines, typical parameters are used as available for the National Power Grid in Poland [31]. For modeling of the transmission line single-circuit sections, line towers of the Y52P type are assumed, while for the double-circuit, line towers of the Z52P type are assumed. The ferroresonant circuits are created due to maloperation of a circuit breaker as a consequence of switching off operation of the long transmission line terminated with an

autotransformer (the autotransformer is located at the end of Line B). In the all analyzed scenarios the examined operation of the circuit breaker was assumed as two phase deenergization of Line B (which assumes the event of the circuit breaker maloperation). The opening time of the breaker was simulated at 0.4 s.

Table 1. Parameters of electrical components used in simulation model of test system

Element	Parameters
Voltage sources	U = 420 kV, S''_K = 1 GVA for B5 and 3 GVA for B1 F = 50 Hz
Autotransformers	S_n = 330 MV 410/123/15.65 kV
Lines	Single-circuit sections: 75 km (tower type Y52P) Double-circuit section: 25 km, 50 km, 75 km or 100 km (tower type Z52P)
Loads	0 MW, 0 Mvar

The short-circuit power at the system nodes was defined with the use of the voltage source and the equivalent Thévenin circuit impedance. For modeling ferroresonant power system transients the frequency dependent models of transmission lines were used.

The developed model of the test system allows one to study variety of ferroresonant configurations, including also those with series and shunt compensated lines not depicted in Fig. 5 (i.e. requiring adding the reactors model to the model outlined).

5.2. Simulation scenarios

In the study presented in this paper the impact of the parameters of the overhead transmission line is examined on occurrence and mode of the ferroresonance phenomenon. The ferroresonance was analyzed for the assumed test system for different lengths of the mutual connection of the multi-circuit transmission line (providing the critical for ferroresonance interaction between components). The length of the double-circuit segment between points B2–B3 was assumed as follows: 25 km, 50 km, 75 km or 100 km. Two-phase switching operation of the circuit breaker at node B5 was simulated to initiate ferroresonance in the analyzed circuit. Table 2 summarizes the investigated study cases.

Fig. 6 shows an example of a voltage waveform at node B6 obtained for a segment of a double-circuit transmission line of 25 km in length (see Case 1 in Table 2). Length of each segment of the single-circuit line is 75 km.

For analyzing the ferroresonance waveforms three consecutive periods can be distinguished. Period 1 comprises of the waveform in the pre-fault steady state. It lasts until the occurrence of the switching process. Period 2 starts at the time of the occurrence of switching operation and lasts until the sustained ferroresonance is established.

The ferroresonant waveform during Period 2 is related to the transient state, i.e. the waveform can be characterized with crest value that is different for each ferroresonance event. Period 3 starts

Table 2. Ferroresonance study cases in investigated high voltage 400 kV system

Study case	Length of transmission line segment		Number of wires and cross section of wires bundle in transmission line
	l_{B1-B2}, l_{B5-B2}, l_{B3-B4}, l_{B3-B6}	l_{B2-B3}	
Case 1	75 km	25 km	2×525 mm^2
Case 2		50 km	2×525 mm^2
Case 3		75 km	2×525 mm^2
Case 4		100 km	2×525 mm^2

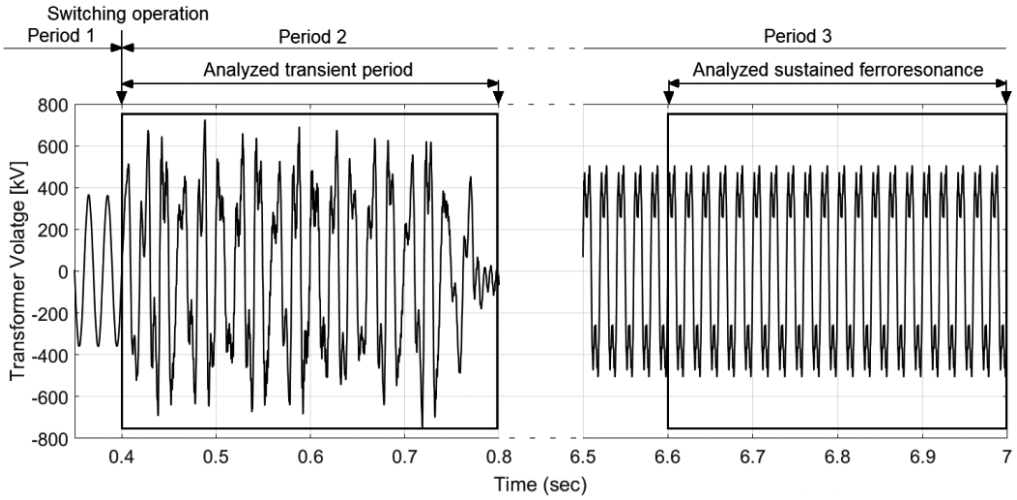

Fig. 6. Analyzed parts of voltage waveforms after switching operation (transient phase) and in sustained ferroresonance phase, obtained for the simulation model with 25 km double-circuit section of overhead line (see Table 2, Case 1)

right after Period 2. It is characterized with a harmonic content, whereas each of the harmonic component has a constant amplitude. This period is also called a sustained ferroresonance. In the case of a single harmonic component, the waveform can be characterized as non-ferroresonant.

For the simulation results obtained in the work reported in this paper, two parts of the voltage waveforms were analyzed:

– For Period 2: the transient part of the waveforms, due to switching operation according to description given above, from 0.4 s to 0.8 s,
– For Period 3: the sustained ferroresonance part of the waveforms (or non-ferroresonant waveform) according to description given above, from 6.6 s to 7.0 s).

To identify different types of ferroresonance, the approach based on Poincaré maps was used. Fig. 7 shows the obtained Poincaré maps for four variants of the simulated system according to Table 2. The Poincaré maps obtained for Period 2 of the process is denoted with squares

indicating transient ferroresonance state (i.e. after two-phase operation of the circuit breaker). Then, the Poincaré maps obtained for Period 3 of the process is denoted with circles indicating sustained ferroresonance state.

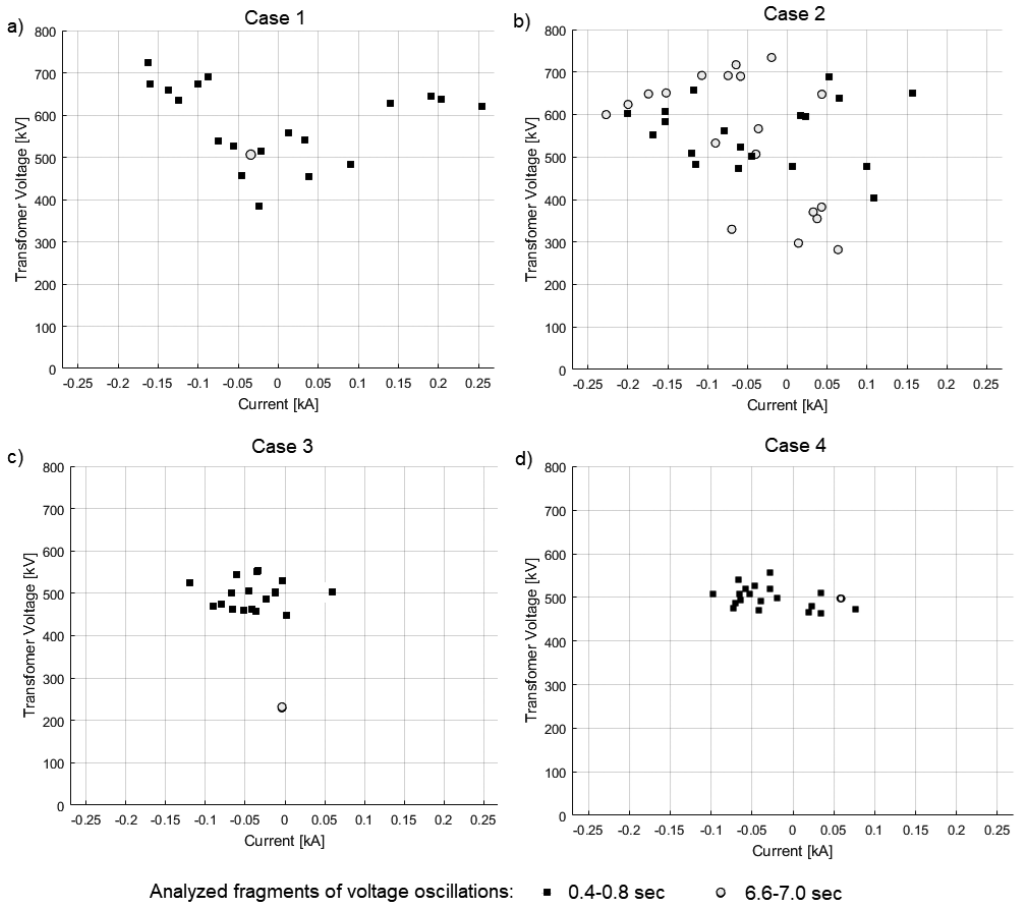

Fig. 7. Results of ferroresonance analysis with Poincaré maps for different length of double-circuit transmission line (study cases according to Table 2: Case 1 – 25 km (a); Case 2 – 50 km (b); Case 3 – 75 km (c); Case 4 – 100 km (d)) and for two periods of the ferroresonance waveforms (squares for Phase 1 after switching operation, circles for Phase 2 of sustained ferroresonance)

Based on the simulation results performed for the system model as shown in Fig. 5 and based on the analyses performed for the simulated voltage and current waveforms with the Poincaré maps approach as shown in Fig. 7, it can be concluded that the length of the double-circuit line has a significant impact on the ferroresonance type and severity. Particularly, the length of the double-circuit section can have a critical impact on whether the ferroresonance is of a transient or sustained type.

In Study Case 1 (see Table 2, a double-circuit line length of 25 km), after two-phase switching operation of the circuit breaker, the ferroresonance waveforms are of a chaotic type, while in the sustained period the waveforms are built with basic harmonic components. Hence, it can be stated, that during the ferroresonance process the type of the oscillations constituting the process can vary with time.

In the case when the analyzed waveform is of a periodic type, only one point is observed in the Poincaré map (see Fig. 7(a, c, d)) for the time range after the sustained ferroresonance state is established. The results of simulations reported here for the simulation case with a double-circuit transmission line of 50 km in length (see Table 2, Case 2) indicate that the entire analyzed waveform has varying crest voltage, which is illustrated in Fig. 7(b). This feature is due to the occurrence of the Transient Overvoltages (TOVs), which are of different amplitudes during the time span of interest.

For a double-circuit line of 75 km in length (see Table 2, Case 3), after switching operation the ferroresonance of a chaotic character is observed, whereas the ferroresonance is attenuated after a steady state is established. Fig. 7(c) shows that after two-phase switching the ferroresonance becomes of a chaotic type, however the points in the Poincaré map are mostly concentrated in a specific area. This indicates that the ferroresonance oscillations are close to a harmonic type.

For a double-circuit line of 100 km in length (see Table 2, Case 4), after two-phase switching operation of the circuit breaker, the ferroresonance becomes of a chaotic type. After a steady state is established, the oscillations become of a harmonic type, with constant amplitude.

5.3. Impact of double-circuit transmission line tower design

To investigate an impact of a double-circuit transmission line tower design on the ferroresonance phenomenon, a comparative study has been conducted for two typical line tower designs. Fig. 5 shows the assumed system topology, in which the line segment l_{B2-B3} was assumed as the line tower of type Z52P and E33. The assumed line tower structures are shown in Fig. 8. For analyzing the ferroresonance, the peak voltage $V_{\max}$ was calculated at node B6 (the line ended with autotransformer). This voltage was used as a criterion to indicate the ferroresonance condition in the analyzed system. The system was analyzed for different values of the line l_{B2-B3} segment length. For initiating ferroresonance in the analyzed system, a two-phase operation of a circuit breaker was simulated. The circuit breaker operated in the power transformer supplying the transmission line. Table 3 shows the simulation results indicating that the $V_{\max}$ value strongly depends on the design of the transmission line tower, which thus has an impact on the ferroresonance condition. The impact of the tower line design on the ferroresonance occurrence depends on the

Table 3. Comparison of peak voltage $V_{\max}$ during ferroresonance for two transmission line towers

Transmission line tower design	$\boldsymbol{V_{\max}}$ [kV]			
	l_{B2-B3} = 25 km	l_{B2-B3} = 50 km	l_{B2-B3} = 75 km	l_{B2-B3} = 100 km
Z52P	732	755	787	803
E33	760	740	815	799

double-circuit transmission line segment (l_{B2-B3}) length. This means that the peak voltage $V_{\max}$ occurs for different line segments l_{B2-B3} of Z52P and E33 designs, which is yet another aspect of complexity of the ferroresonance phenomenon.

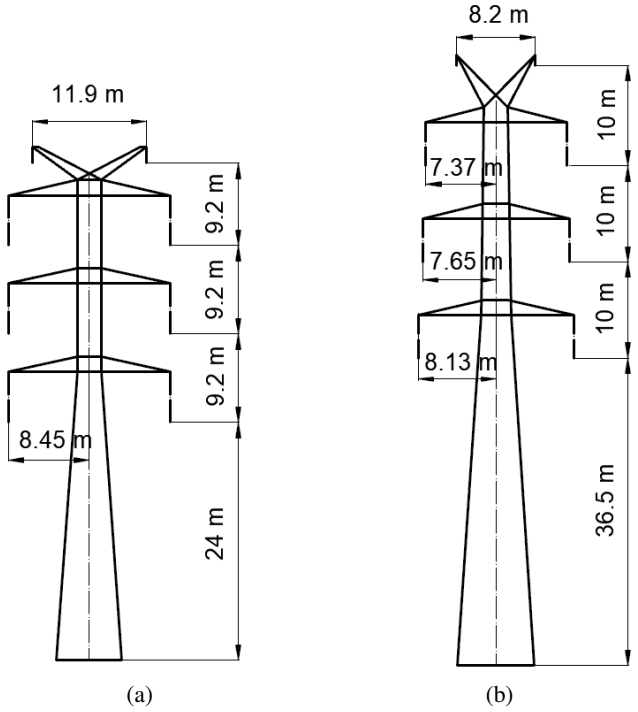

(a) (b)

Fig. 8. Design structure for towers with dimensions: Z52P (a); E33 (b)

The analysis of different double-circuit transmission line tower designs indicates the chaotic behavior of ferroresonance for all analyzed cases during Period 2 (after switching operation). The maximum overvoltage values occur during this Period (according to the Table 3). The Poincaré maps obtained for Z52P (squares) and E33 (circles) of the sustained ferroresonance state (Period 3) are presented in Fig. 9. The analysis of Period 3 (Fig. 9) indicates that subharmonic ferroresonant types were obtained for shorter line lengths – 25 km and 50 km for both Z52P and E33 transmission line tower designs. However, ferroresonant waveforms differ in shape and amplitude. Therefore, points on the Poincaré maps in Cases 1 and 2 are in different positions. In turn, for a double-circuit line of 75 km and 100 km in length (see Fig 9, Case 3 and 4), the ferroresonant oscillations become of a fundamental type, with constant amplitude. The analysis of Table 3 and Poincaré maps in Fig. 9 show that different values of overvoltages are obtained for different line lengths and different transmission line tower designs. This study highlight that tower design as well as transmission line length have influence on the ferroresonance phenomenon. From the point of view of ferroresonance, it is necessary to analyze the different possible transmission line tower design for a particular length of the line. One type of transmission towers may be better for shorter lengths and another type for longer lengths of overhead lines.

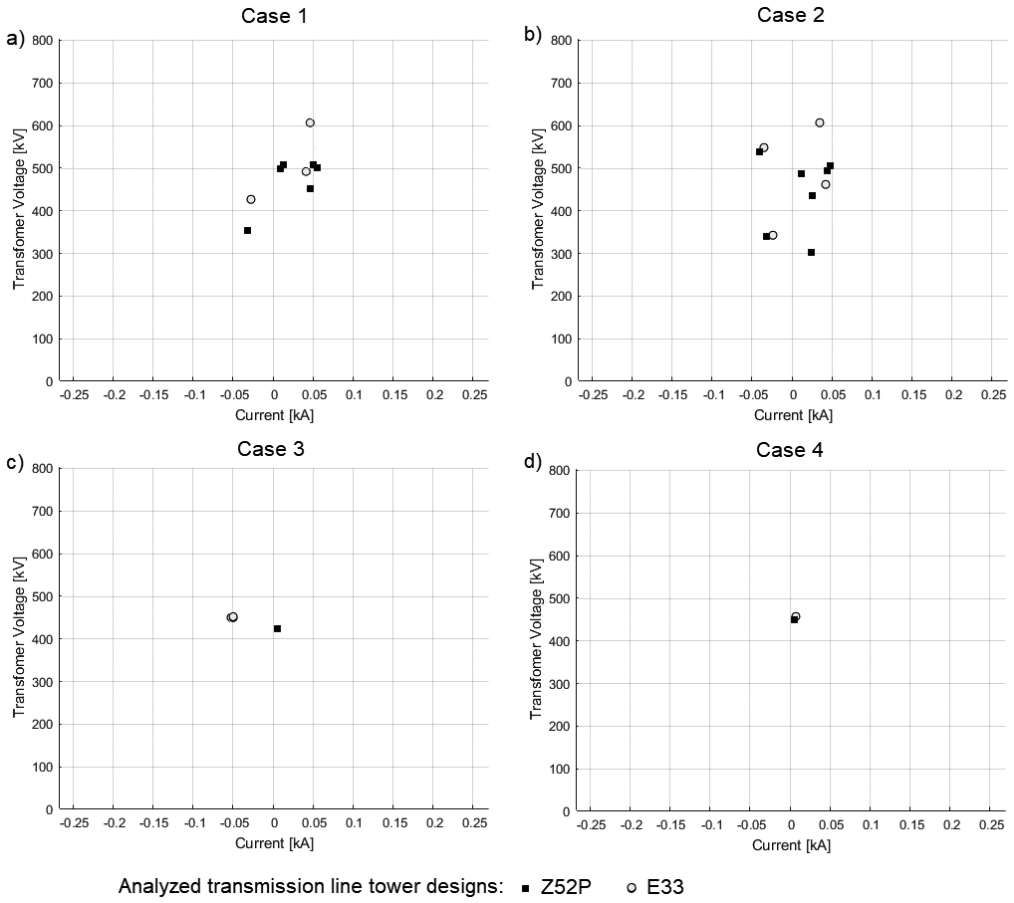

Fig. 9. Results of sustained ferroresonance analysis with Poincaré maps for different length of double-circuit transmission line (study cases according to Table 3: Case 1 – 25 km (a); Case 2 – 50 km (b); Case 3 – 75 km (c); Case 4 – 100 km (d)) and for two transmission line tower designs: Z52P (squares) and E33 (circles)

6. Conclusions

In this paper the analysis of the ferroresonance phenomenon was reported for a typical high voltage 400 kV test system. Ferroresonance was analyzed for several study cases of double-circuit line length (constituting for system capacitance) and of a power transformer (constituting for non-linear inductance). The analyses were performed with the use of the simulation model developed in the PSCAD simulation software. The presented analyses are motivated with the constant need to analyze the ferroresonant conditions for constantly changing structure of a power grid. Based on the simulation results presented it can be concluded that the length of the transmission lines involved in ferroresonance generation has a significant impact on the ferroresonance occurrence and on its type. The ferroresonance can be initiated when a transmission line, that is incoming to

the power station terminated with power transformer, is de-energized by two-phase operation of a circuit breaker. The type of the ferroresonance depends on the length of the transmission line that is mutually coupled in a double-circuit transmission line arrangement. Moreover, the type of the ferroresonance can change after being initiated.

Among variety of approaches that are in use for analyzing of the ferroresonance phenomenon, the Poincaré maps approach was found useful in this paper. The simulation results were presented for a typical variant of the test system configuration, which allows one to conclude that using the Poincaré map is an effective method for analyzing the ferroresonance occurrence and its type. It also allows for the classification of the ferroresonance type and to calculate the crest values of the ferroresonant overvoltages.

The system scenarios assumed in this paper are of importance for present grid developments and modernization work, as currently announced or conducted by the national grid operator in Poland. Such development work requires system studies, including ferroresonance, for which the impact of double-circuit transmission lines design on ferroresonance is considered as a critical part. The results presented in this paper allow further investigation of the impact of the tower design on the occurrence and severity of the ferroresonance phenomenon.

References

[1] Jacobson D., *Examples of Ferroresonance in a High Voltage Power System*, IEEE Power Engineering Society 2003 General Meeting, Toronto, Ontario, Canada, vol. 2, no. 3, pp. 1206–1213 (2003).

[2] Bolkowski S., *Theory of Electrical Circuits*, Wydawnictwa Naukowo-Techniczne (in Polish) (1995).

[3] Karolak J., Przybysz J., Wiśniewski J., *Ferroresonance phenomena in high voltage substations*, Przegląd Elektrotechniczny (in Polish), vol. 93, no. 11, pp. 79–83 (2017).

[4] Tarko R., Benesz M., Makuch A., Szpyra W., Nowak W., *Ferroresonance as a source of disturbances and failures in medium voltage distribution grids*, Acta Energetica, vol. 4, no. 9, pp. 75–82 (2011).

[5] Jacobson D., *Examples of Ferroresonance in a High Voltage Power System*, in 2003 IEEE Power Engineering Society General Meeting, Toronto, Ontario, Canada (2003).

[6] Abdi H., Abbasi S., Moradi M., *Analyzing the stochastic behavior of ferroresonance initiation regarding initial conditions and system parameters*, Electrical Power and Energy Systems, vol. 83, pp. 134–139 (2016).

[7] Jacobson D., Menzies R.W., *Investigation of Station Service Transformer Ferroresonance in Manitoba Hydro's 230-kV Dorsey Converter Station*, International Conference on Power Systems Transients 2001 (IPST 2001), Rio de Janeiro, Brazil, pp. 1–6 (2001).

[8] Tugai I., *Investigation of ferroresonance in electrical networks at open-phase operating conditions*, Computational Problems of Electrical Engineering, vol. 5, no. 1, pp. 61–64 (2015).

[9] Abdallah A.S., El-Kady M.A., *Ferroresonance Phenomenon in Power Transformers – Experimental Assessment*, Journal of King Abduaziz University (JKAU) Engineering Science, vol. 16, no. 1, pp. 71–82 (2005).

[10] Jacobson D., Marti L., Menzies R.W., *Modeling Ferroresonance in a 230 kV Transformer-Terminated Double-Circuit Transmission Line*, International Conference on Power system Transients 1999 (IPST 1999), Budapest, Hungary, pp. 451–456 (1999).

[11] Majka L., *Applying a fractional coil model for power system ferroresonance analysis*, Bulletin of the Polish Academy of Sciences: Technical Sciences, vol. 66, no. 4, pp. 467–474 (2018).

[12] Kolańska-Płuska J., Grochowicz B., *Modelling of a non-linear coil with loss in iron using the Runge-Kutta methods*, Archives of Electrical Engineering, vol. 65, no. 3, pp. 527–539 (2016).

[13] Szewczyk M., Kutorasiński K., Pawłowski J., Piasecki W., Florkowski M., *Advanced modeling of high frequency magnetic cores for damping of power system transients*, IEEE Transactions on Power Delivery, vol. 31, no. 5, pp. 2431–2439 (2016).

[14] Szewczyk M., Kuczek T., Oramus P., Piasecki W., *Modeling of repetitive ignitions in switching devices: case studies on Vacuum Circuit Breaker and GIS disconnector*, Lecture Notes in Electrical Engineering, vol. 324, pp. 241–250 (2015).

[15] Barbisio E., Bottauscio O., Chiampi M., Crotti G., Giordano D., *Parameters Affecting Ferroreso-nance in Electric Circuits*, IEEE Transactions on Magnetics, vol. 44, no. 6, pp. 870–873 (2008).

[16] Dugan R.C., McGranaghan M.F., Santoso S., Beaty H.W., *Electrical Power Systems Quality*, McGraw-Hill (2012).

[17] Valverde V., Buigues G., Mazón A.J., Zamora I., Albizu I., *Ferroresonant Configurations in Power Systems*, International Conference on Renewable Energies and Power Quality (ICREPQ'12), Santiago de Compostela, Spain (2012).

[18] Working Group C4.307, *Resonance and Ferroresonance in Power Networks*, Cigre Technical Brochure 569 (2014).

[19] Sandip M., Panwar P., *Ferroresonance: An Insight into the Phenomenon*, International Journal of Advance Engineering and Research Development, vol. 4, no. 10, pp. 498–504 (2017).

[20] Rezaei-Zare S., Sanaye-Pasand M., Mohseni H., Farhangi S., Iravani R., *Analysis of Ferroresonance Modes in Power Transformers Using Preisach-Type Hysteretic Magnetizing Inductance*, IEEE Transactions on Power Delivery, vol. 22, no. 2, pp. 919–929 (2007).

[21] Ang S.P., Peng J., Wang Z., *Identification of key circuit parameters for the initiation of ferroresonance in a 400-kV transmission system*, 2010 International Conference on High Voltage Engineering and Application, New Orleans, USA, pp. 73–76 (2010).

[22] Rezaei S., *Mitigation of Ferroresonance by FACTS In Electrical Network*, International Journal on Electrical Engineering & Informatics, vol. 9, no. 1, pp. 1–23 (2017).

[23] Seker S., Akinci T.C., Taskin S., *Spectral and statistical analysis for ferroresonance phenomenon in electric power systems*, Electrical Engineering, vol. 94, no. 2, pp. 117–124 (2012).

[24] Yildırim S., Akinci T.C., Seker S., Ekren N., *Determination of the characteristics for ferroresonance phenomenon in electric power systems*, World Academy of Science, Engineering and Technology, vol. 55, pp. 108–112 (2009).

[25] Mokryani G., Haghifam M.R., Esmaeilpoor J., *Identification of Ferroresonance Based on Wavelet Transform and Artificial Neural Networks*, 2007 Australasian Universities Power Engineering Conference, Perth, Australia, pp. 1–6 (2007).

[26] Rezaei S., *Impact of plant outage on ferroresonance and maloperation of differential protection in the presence of SVC in electrical network*, IET Generation, Transmission and Distribution, vol. 11, no. 7, pp. 1671–1682 (2017).

[27] Robak S., Szewczyk M., Polewaczyk M., *Ferroresonance in transmission networks – selected issues*, Safety of the Polish Power System Edition 2018, Scientific Publishers OWN, pp. 61–75 (2018).

[28] Kato T., Inoue K., Takami Y., *Stability Analysis using Poincaré map in the Time-Domain for Grid-Connected Inverter*, 2017 IEEE 18th Workshop on Control and Modeling for Power Electronics (COMPEL), Stanford, USA, pp. 1–7 (2017).

[29] Ferracci P., *Ferroresonance*, Group Schneider: Cahier no 190, pp. 1–28 (1998).

[30] PSCAD Power Systems Computer Aided Design – User's Guide on the use of PSCAD, Manitoba HVDC Research Centre (2018).

[31] Maciejewski Z., *Influence of transmission lines on efficiency of the power system*, Polityka Energetyczna – Energy Policy Journal (in Polish), vol. 17, no. 3, pp. 231–242 (2014).